

## Giant Resonances in Cold Electron Scattering by CS<sub>2</sub>

N. C. Jones,<sup>1</sup> D. Field,<sup>1,\*</sup> J.-P. Ziesel,<sup>2</sup> and T. A. Field<sup>3</sup>

<sup>1</sup>*Institute of Physics and Astronomy, University of Aarhus, DK-8000 Aarhus C, Denmark*

<sup>2</sup>*Laboratoire Collisions Agrégats Réactivité (CNRS UMR5589), Université Paul Sabatier, 31062 Toulouse, France*

<sup>3</sup>*Department of Pure and Applied Physics, Queen's University, Belfast BT7 1NN, United Kingdom*

(Received 13 March 2002; published 8 August 2002)

Experimental data are presented for the scattering of cold electrons by CS<sub>2</sub>, for both integral and backward scattering, between a few meV and a few hundred meV impact energy. Giant resonances with cross sections in excess of 50 Å<sup>2</sup> are observed below 100 meV, associated with the transient formation of CS<sub>2</sub><sup>-</sup> at 15 meV and with the bend and symmetric stretch of CS<sub>2</sub> at thresholds of 49 and 82 meV, respectively. The resonance at 49 meV is 2 orders of magnitude greater in cross section than a dipole impulsive model predicts. These structures are superimposed on a sharp rise in the scattering cross section at low energy, which may be attributed to virtual state scattering.

DOI: 10.1103/PhysRevLett.89.093201

PACS numbers: 34.80.Gs, 34.80.Bm, 34.80.My

The scattering and attachment of low energy electrons by atomic and molecular targets exemplify fundamental phenomena of quantum scattering [1–5], such as Feshbach resonances [6], virtual state scattering [7,8], or strong suppression of rotationally inelastic scattering [1,9,10]. The scattering of cold electrons is a subject closely related to cold atom collisions, since de Broglie wavelengths are comparable and interactions tend to be governed by asymptotic long-range potentials [11]. The present work demonstrates qualitatively new behavior in electron scattering, displaying resonances 1 to 2 orders of magnitude greater in cross section than have previously been observed in the low energy regime.

The experimental system has been described in detail elsewhere [7,12]. Synchrotron radiation from the ASTRID storage ring at the University of Aarhus provides a high resolution electron source through threshold photoionization of argon at 15.75 eV. The resulting photoelectrons have an energy resolution which is determined by the energy resolution in the photon beam, set here to ~1.6 meV full width at half maximum. Electrons are formed into a beam and pass through room temperature target gas. The intensity of the electron beam, in the presence and absence of target gas, is recorded as a function of electron energy. This yields the variation with energy of the total integral scattering cross section,  $\sigma_T$ , via  $\sigma_T = (NI)^{-1} \ln(I_0/I_t)$ , where  $N$  is the target gas number density,  $l$  is the path length in the gas, and  $I_0$  and  $I_t$  are, respectively, the intensities of the incident and transmitted electron beams. Electron energies are calibrated by comparison with data for N<sub>2</sub> and at low energies are accurate to  $\pm 1$ – $2$  meV [1]. An axial magnetic field of strength  $\sim 2 \times 10^{-3}$  T may also be introduced. In these separate measurements, only backward scattered electrons are recorded as lost to the incident beam, since forward scattered electrons are guided onto the detector. The cross section measured is the total backward scattering cross section  $\sigma_B$ , that is, the cross section for all events which cause electrons to be scattered into the backward  $2\pi$  sr.

Experimental results are shown in Fig. 1. There are no literature data available for comparison at impact energies shown. At energies above 300 meV, our results (available on request) agree within better than 10% with data in [13] but are a little lower than those in [14] between 500 meV and 1 eV. The most recent theories [15,16] severely underestimate the cross section at low energy, although the results of [16], which extend down to 50 meV, hint at the virtual state process (see below).

While no rigorous analysis is possible because of the obscuring effects of the giant resonances in the scattering spectrum, the general rise in cross section at low energy is likely to be due to virtual state scattering. As discussed in detail in [7,8], the behavior with energy of the ratio  $R = \sigma_B/\sigma_T$  is diagnostic of the sign of the  $s$ -wave scattering length,  $A_0$ , which must be negative for the virtual state process. The value of  $R$  as a function of electron energy is shown in Fig. 2 and is seen to be less than 0.5 at higher energies and to rise towards the limiting value of 0.5 at the

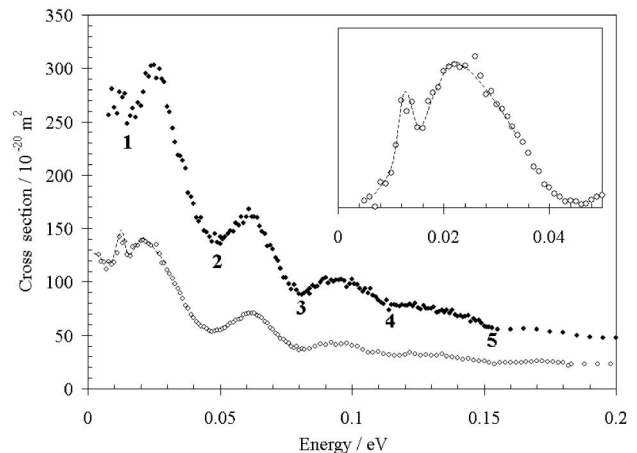


FIG. 1. Integral (upper set) and backward cross sections (lower set) for scattering of electrons by CS<sub>2</sub> as a function of electron impact energy. The inset shows the low energy backward scattering data with the background removed (see text).

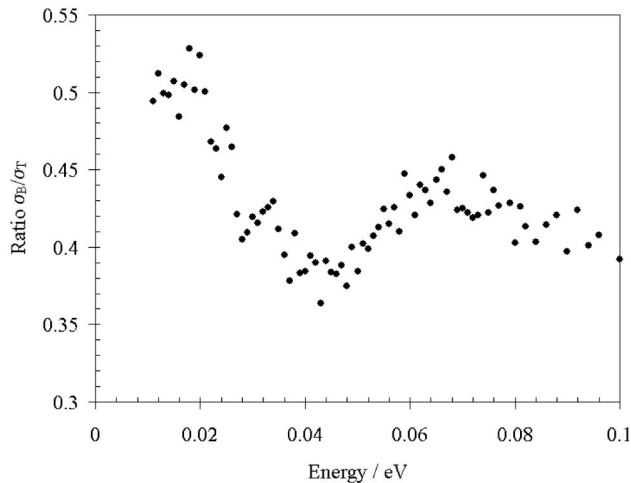


FIG. 2. The ratio of the backward to integral scattering cross sections,  $R$ , as a function of electron impact energy.

lowest energies shown. As explained in [7,8], this suggests that  $A_0$  is indeed negative. Virtual state scattering also requires that the negative ion of the target should be unbound to autodetachment in the equilibrium geometry of the neutral and that the target molecule should be able to form, through structural rearrangement, a negative ion that is stable to nonadiabatic electron detachment. Results in [17] show that  $\text{CS}_2$  satisfies these conditions. According to [17], in linear geometry the energy of  $\text{CS}_2^-$  lies  $\sim 100$  meV above the neutral.  $\text{CS}_2^-$  becomes stable to nonadiabatic detachment on bending through only  $\sim 10^\circ$ . The absence of a bound state in linear geometry is supported by Rydberg atom collisional data [18,19]. The experimental adiabatic electron affinity of  $\text{CS}_2$  lies between 0.5 [20] and 0.9 eV [21], reflecting the existence of a stable, bent form of  $\text{CS}_2^-$ .

We turn now to the giant resonances in Fig. 1. Our goal is a qualitative understanding based upon arguments in terms of symmetry.  $\text{CS}_2$  belongs to the  $D_{\infty h}$  point group, and the ground electronic state of  $\text{CS}_2$  is of  $^1\Sigma_g^+$  symmetry. The lowest unoccupied molecular orbital is  $\pi_u$ , and therefore the linear form of  $\text{CS}_2^-$  is of  $^2\Pi_u$  symmetry. Renner-Teller splitting, lowering the symmetry to  $C_{2v}$ , forms the ground  $^2A_1$  state and an excited  $^2B_1$  state, degenerate only in the linear configuration. The symmetric stretch and bending vibrations of  $\text{CS}_2$  undergo a Fermi resonance [22]. For simplicity, the small effects of Fermi resonance and also of the small thermal populations of excited vibrational states are ignored in the analysis which follows.

The three fundamental vibrational modes of  $\text{CS}_2$  [13] lie at energies of 49, 81, and 190 meV, respectively, for the bending vibration, of  $\Pi_u$  symmetry, the symmetric stretch, of  $\Sigma_g^+$  symmetry, and the asymmetric stretch of  $\Sigma_u^+$  symmetry. In the bent form of  $\text{CS}_2^-$ , the vibrations are, respectively, of symmetry  $A_1$ ,  $A_1$ , and  $B_1$ .

We proceed by considering vibrational excitation without electronic effects, that is, without temporary negative

ion (TNI) formation. For symmetry-allowed vibrational excitation by electron impact, the product of the incoming and outgoing representations ( $\Gamma$ ) of the partial waves must have an irreducible representation the same as that of the vibration involved, that is,  $\Gamma_{\text{in}}\Gamma_{\text{out}}$  must equal  $\Gamma_{\text{vib}}$ . With respect to rotational changes, the symmetry does not change on undergoing a transition and thus the products of the representations are always totally symmetric and do not affect our analysis. A straightforward analysis shows that combinations of  $s$  and  $p_x, p_y$  may excite the bend of  $\text{CS}_2$  and that incoming and outgoing  $s$  and  $p_z$  wave combinations may excite the asymmetric stretch.

The resonance labeled 2 in Fig. 1 has a threshold at 49 meV and is clearly associated with the bend of  $\text{CS}_2$ . Using standard expressions for the first-order Born point-dipole cross section [23] and known line strengths [24], the maximum value of the Born integral inelastic scattering cross section is  $0.45 \text{ \AA}^2$ , whereas the cross section associated with the resonance in the data is greater than  $50 \text{ \AA}^2$ . A typical measured integral cross section for vibrationally inelastic scattering is of the order of a few  $\text{ \AA}^2$ , noting that agreement with the first-order Born point-dipole model is generally within a factor of 2 or better [25]. These considerations rule out a Born impulsive process as the origin of the 49 meV feature. The resonance labeled 3 in Fig. 1 has a threshold of 82 meV and is therefore clearly associated with the Raman symmetric stretch, which cannot be excited by a dipole mechanism. By contrast, a weak feature is detectable with a measured onset of 188 meV, which corresponds to Born-type excitation of the asymmetric stretch [13].

The above considerations prompt the question of whether temporary attachment could provide an explanation for the giant resonances in Fig. 1. The finite lifetime of the TNI requires that the electron-molecule encounter be represented as a superposition of paths, some of which explore the regime in which the target is essentially linear, in  $D_{\infty h}$  symmetry, and some in which the system is better described in  $C_{2v}$  symmetry.  $D_{\infty h}$  symmetry for the TNI is first considered in the symmetry analysis described below. Since the TNI undergoes vibronic coupling to lower the symmetry through the Renner-Teller effect, the phenomenon of attachment must be treated as a vibronic rather than a purely electronic process [12]. Thus, in order to treat the symmetry in attachment to  $\text{CS}_2$ , it is necessary to include the symmetry of vibrations excited in the TNI.

All combinations of  $s, p_x, p_y, p_z$  waves as input and output waves and all situations of elastic scattering and vibrational excitation of the product have been considered, including all paths which involve vibrational excitation of the TNI (but without overtones). The effective number of possible channels is reduced since, under  $D_{\infty h}$  symmetry,  $p_x$  and  $p_y$  are indistinguishable. The double requirement is invoked that both attachment and overall vibrational excitation be symmetry allowed. Two examples

illustrate the method. With a  $p_{x,y}$  wave on the input channel and an  $s$  wave on the output channel, no intermediate excitation of the TNI, but with bend excitation in the final state of  $\text{CS}_2$ , the attachment process is represented by an integrand of symmetry  $\Pi_u \Pi_u \Sigma_g^+$ . This has an irreducible representation which is totally symmetric ( $\Sigma_g^+$ ) and therefore attachment is feasible. The purely vibrational part is also  $\Pi_u \Pi_u \Sigma_g^+$  in this case, and therefore again represents a symmetry-allowed process. The process is therefore overall symmetry allowed. A counterexample is one in which (for example) a  $p_x$  wave enters, without excitation in the TNI and exits as an  $s$ -wave, exciting an asymmetric vibration in  $\text{CS}_2$ . In this case the attachment process is feasible, represented by the product of  $\Pi_u \Pi_u \Sigma_g^+$ . The excitation process is, however, represented by  $\Pi_u \Sigma_u^+ \Sigma_g^+$ , which is overall  $\Pi_g$  and therefore a forbidden channel.

Conclusions from this analysis may be summarized as follows.  $s$ -wave scattering in both input and exit channels may, via vibronic effects mentioned above, be either elastic or give rise to excitation of the symmetric stretch in  $\text{CS}_2$ .  $p_{x,y}$  waves show the same behavior.  $s$  waves in the input channel and  $p_{x,y}$  waves in the output channel, or vice versa, can give rise to excitation of the bending vibration in  $\text{CS}_2$ . No process can give rise to excitation of the asymmetric stretch via attachment.

We now include trajectories in which the system is described in  $C_{2v}$  symmetry, that is, the target is sufficiently bent that it is adiabatically stable to electron loss. The incoming wave is therefore treated as if moving in a field of  $C_{2v}$  symmetry. The outgoing channel remains that for the linear molecule, since only for the (almost) linear species is electron loss an open channel. Scattering takes place on a superposition of  ${}^2A_1$  and  ${}^2B_1$  surfaces. There are difficulties involved in treating a dynamical process in which the symmetry changes in the course of the interaction, since it is naturally not possible to form the direct product between the representations of two different point groups. However, the TNI, formed in a  $C_{2v}$  dominated environment, subsequently samples the  $D_{\infty h}$  environment, in order to couple into the  $\text{CS}_2$  plus free electron output channel. Thus  $B_1$  evolves into  $\Pi_u$ , and the  $A_1$  symmetry of the incoming  $s$  wave is equivalent in the output channel to  $\Sigma_g^+$ .

The conclusions are in fact little different from the previous analysis, save that only  $p_x$  waves can be active in scattering, and that processes may be divided into those which involve either the ground  ${}^2A_1$  state or the excited  ${}^2B_1$  state. On the  ${}^2A_1$  surface,  $s$  waves behave as described previously. For example,  $s$  waves on the input channel and  $p_x$  on the output yield bending excitation of  $\text{CS}_2$ . On the  $B_1$  surface,  $p_x$  waves on both the input and output channels can give rise to both elastic scattering and symmetric stretch excitation of  $\text{CS}_2$ .  $p_x$  waves on the input channel and  $s$  waves on the output channel, again on the  $B_1$  surface, can give rise to bending excitation of  $\text{CS}_2$ .

Symmetry arguments demonstrate that (i) scattering associated with the bending vibration, be it elastic or inelastic, may be coupled to the attachment channel. We would suggest that this is the origin for the giant resonance observed at a threshold of 49 meV. (ii) The Raman allowed symmetric vibrational mode, otherwise expected to be inactive in the scattering, is also coupled to the attachment channel above the threshold at 82 meV. A simple physical picture is that attachment symmetrically lengthens the C-S bond length by  $\sim 0.075 \text{ \AA}$  [17]. The molecule therefore expands during the collisional lifetime, equivalent to nuclear-electronic coupling into the symmetric stretch. (iii) The asymmetric stretch is not involved in scattering via attachment. This is why the feature associated with the asymmetric stretch at 188 meV is weak. The Born-type process exciting this mode has an observed and a calculated cross section [13,23] of a few  $\text{\AA}^2$  in the integral cross section and  $\sim 1 \text{ \AA}^2$  in the backward cross section.

Our analysis also serves qualitatively to explain the variation of the backward to integral scattering cross sections,  $R$ , shown in Fig. 2. As energy increases towards the threshold for the bend (49 meV), the value of  $R$  drops, as expected for virtual state scattering. Beyond this threshold, the value of  $R$  rises sharply. According to symmetry arguments, the outgoing waves associated with scattering, involving the bending vibration, are  $s$ ,  $p_x$ , and  $p_y$ . These waves give rise to backward-forward symmetry. The variation of  $R$  in fact follows the form of the rise and fall of the resonance associated with the bend, showing behavior consistent with the model of attachment discussed above.

Turning to feature 1 of Fig. 1, this lies below threshold for any vibrationally inelastic process associated with  $\text{CS}_2$ . The backward scattering data show that peak 1 is clearly a doublet, with peak separation  $11 \pm 1$  meV. The energies of the peaks lie at  $13 \pm 0.5$  meV and  $24 \pm 0.5$  meV. The width of the peaks are, respectively, 3.5 and 13 meV, figures obtained by fitting the wing of a Gaussian to the underlying background and a Gaussian to each of the peaks (see inset in Fig. 1). We suggest that peak 1 arises through vertical electron attachment into the linear form of  $\text{CS}_2^-$ , consistent with the very small energy separation calculated in [17]. Our experimental energy includes, of course, the difference in zero point energies in  $\text{CS}_2$  and  $\text{CS}_2^-$ , which reduces the expected energy to below the value of  $\sim 100$  meV in [17]. The doublet would then represent the two halves of the spin-orbit states of linear  $\text{CS}_2^-$ . The peak separation is equal to the spin-orbit coupling constant,  $A$ , less  $2B$ , where  $B$  is the rotational constant of  $\text{CS}_2^-$  [26,27]. The correction due to  $B$  is negligible and therefore  $A = 11 \pm 1$  meV or  $89 \pm 9 \text{ cm}^{-1}$ .

While the many rotational populations involved in the scattering obscure the true widths of the two features of peak 1, it remains evident that the lifetime associated with the lower energy peak is almost 4 times greater than that of the higher energy peak. An explanation for this may rest both upon statistical weights and impact energies. If our

interpretation is correct, the peak at 13 meV corresponds to the  ${}^2\Pi_{1/2}$  component and that at 24 meV to the  ${}^2\Pi_{3/2}$  component. An argument based upon statistical weights would therefore suggest that the 13 meV component might decay into the electron plus  $\text{CS}_2$  continuum with half the rate of the 24 meV component. The energy dependence of the lifetime may be expected to follow  $E^{-3/2}$  [28] for those trajectories which may be associated with the  $p$  wave. This would introduce a further factor of 2.5 shorter lifetime for the 24 meV resonance. In fact, the lifetime depends critically on the time spent within the range of bending angles ( $\pm 10^\circ$ ) in which adiabatic electron loss is possible and the simple ideas mentioned here require detailed theoretical investigation.

There remain two readily identifiable features, with thresholds at 116 and 154 meV, each with an integral scattering cross section of  $\sim 5 \text{ \AA}^2$  and with  $R \sim 0.5$ . These threshold energies do not represent overtones or combinations of  $\text{CS}_2$  normal modes. The angular dependence suggests quite strong involvement of  $s$  or  $p_{x,y}$  waves. By analogy with scattering in  $\text{O}_2$  [26], it would seem likely that these resonances are associated with vibrationally excited states of  $\text{CS}_2^-$ . Lower energy members of the series are obscured by the giant resonances.

In conclusion, our data show giant resonances whose energy spectrum may be explained on the basis of symmetry arguments and known properties of  $\text{CS}_2$  and  $\text{CS}_2^-$ . Theoretical models should now address the problem of the remarkable magnitude of the resonances and the proportion of elastic and inelastic scattering which they represent.

We thank the Director and staff of the Institute for Storage Ring Facilities at the University of Aarhus for making this work possible. J. P. Z. would like to thank the CNRS (France) and the SNF (Denmark) for support under the European Science Exchange program. N. C. J. would also like to thank the SNF for support.

---

\*Corresponding author.

Email address: dfield@ifa.au.dk

- [1] D. Field, S. L. Lunt, and J.-P. Ziesel, *Acc. Chem. Res.* **34**, 291 (2001).  
 [2] A. Chutjian, A. Garscadden, and J. M. Walhedra, *Phys. Rep.*, **264**, 393 (1995).

- [3] D. Klar, M.-W. Ruf, and H. Hotop, *J. Phys. B* **34**, 3855 (2001).  
 [4] C. Desfrancois *et al.*, *J. Chem. Phys.* **111**, 4569 (1999).  
 [5] R. Parthasarathy, L. Suess, S. B. Hill, and F. B. Dunning, *J. Chem. Phys.* **114**, 7962 (2001).  
 [6] E. Leber, S. Barsotti, J. Bommels, J. M. Weber, I. I. Fabrikant, M.-W. Ruf, and H. Hotop, *Chem. Phys. Lett.* **325**, 345 (2000).  
 [7] D. Field, N. C. Jones, S. L. Lunt, and J.-P. Ziesel, *Phys. Rev. A* **64**, 22708 (2001).  
 [8] D. Field, J.-P. Ziesel, S. L. Lunt, R. Parthasarathy, L. Suess, S. B. Hill, F. B. Dunning, R. R. Lucchese, and F. A. Gianturco, *J. Phys. B* **34**, 4371 (2001).  
 [9] D. Field, N. C. Jones, S. L. Lunt, J.-P. Ziesel, and R. J. Gulley, *J. Chem. Phys.* **115**, 3045 (2001).  
 [10] S. L. Lunt, D. Field, N. C. Jones, J.-P. Ziesel, and R. J. Gulley, *Int. J. Mass Spectrom.* **205**, 197 (2001).  
 [11] J. Weiner, V. S. Bagnato, S. Zilio, and P. Julienne, *Rev. Mod. Phys.* **71**, 1 (1999).  
 [12] R. J. Gulley, S. L. Lunt, J.-P. Ziesel, and D. Field, *J. Phys. B* **31**, 2735 (1998).  
 [13] W. Sohn, K.-H. Kochem, K. M. Scheuerlein, K. Jung, and H. Ehrhardt, *J. Phys. B* **20**, 3217 (1987).  
 [14] C. Szmytkowski, *J. Phys. B* **20**, 6613 (1987).  
 [15] M. H. F. Bettega, *Aust. J. Phys.* **53**, 785 (2000).  
 [16] M. T. Lee, S. E. Michelin, T. Kroin, and E. Vettenheimer, *J. Phys. B* **32**, 3043 (1999).  
 [17] G. Gutsev, R. J. Bartlett, and R. N. Compton, *J. Chem. Phys.* **108**, 6756 (1998).  
 [18] A. Kalamarides, C. W. Walter, K. A. Smith, and F. B. Dunning, *J. Chem. Phys.* **89**, 7226 (1998).  
 [19] C. Desfrancois, N. Khelifa, J. P. Schermann, T. Kraft, M.-W. Ruf, and H. Hotop, *Z. Phys. D* **27**, 363 (1993).  
 [20] B. M. Hughes, C. Lifshitz, and T. O. Tiernan, *J. Chem. Phys.* **59**, 3162 (1973).  
 [21] J. M. Oakes and G. B. Ellsion, *Tetrahedron* **42**, 6263 (1986).  
 [22] S. Montero, C. Domingo, F. Wetzel, H. Finsterhölzl, and H. W. Schrotter, *J. Raman Spectrosc.* **15**, 380 (1984).  
 [23] J. Randell, J.-P. Ziesel, S. L. Lunt, G. Mrotzek, and D. Field, *J. Phys. B* **26**, 3423 (1993).  
 [24] D. M. Bishop and L. M. Cheung, *J. Phys. Chem. Ref. Data* **11**, 199 (1982).  
 [25] G. A. Gallup, *J. Phys. B* **23**, 2383S (1990).  
 [26] D. Field, G. Mrotzek, D. W. Knight, S. L. Lunt, and J.-P. Ziesel, *J. Phys. B* **21**, 171 (1988).  
 [27] F. Fiquet-Fayard, *J. Phys. B* **8**, 2880 (1975).  
 [28] R. G. Newton, *Scattering Theory of Waves and Particles* (Springer-Verlag, New York, 1982), 2nd ed.